Supporting Information

Conformational states of nucleic acid-peptide complexes monitored by acoustic wave propagation and molecular dynamics simulation

Jonathan S. Ellis[a] and Michael Thompson*[a,b]

[a] Institute of Biomaterials and Biomedical Engineering, 164 College Street, University of Toronto, Toronto, Canada.
[b] Department of Chemistry, 80 St. George Street, University of Toronto, Toronto, ON, Canada; E-mail: mikethom@chem.utoronto.ca.

Table of Contents

I   General Remarks

This Supporting Information document contains images and tabulated datasets referred to in the article that may be of interest to the reader. The first two images are molecular diagrams of docked structures used as the starting conformations for the Molecular Dynamics (MD). The remaining images display various results from the MD simulations. The tables show the complete datasets and modelling solution sets that are summarised in the paper.

II Figures
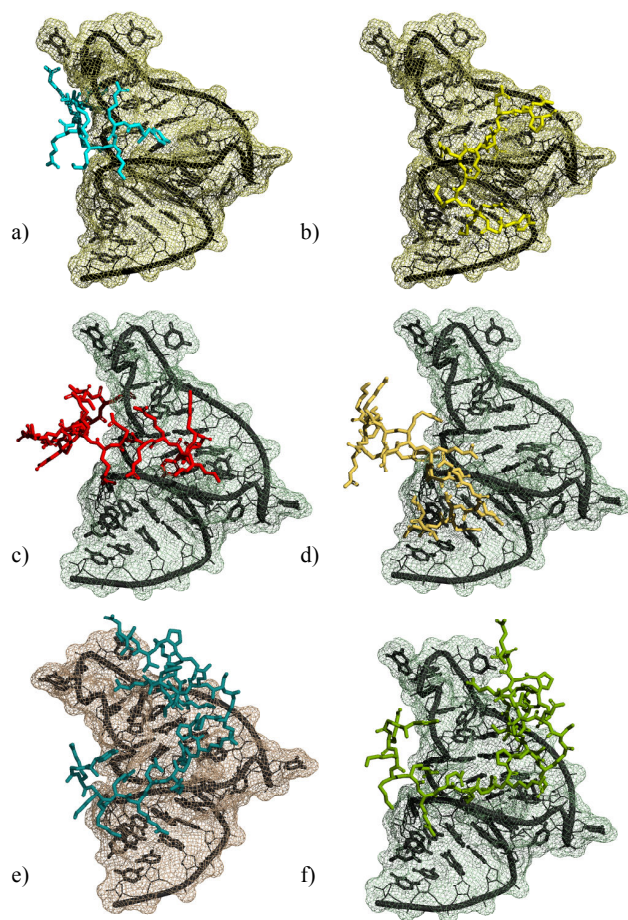
Fig. S.1 - Docked structures showing locations of *Tat* peptide and TAR RNA. The Van der Waals surface is displayed for clarity. The structures are a) 12.3, b) 12.12, c) 22.15, d) 22.18, e) 30.1, and f) 30.18.
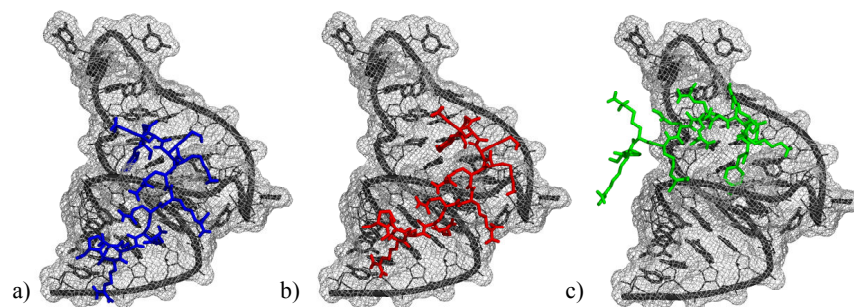
Fig. S.2 - Diagrams showing location of the different lowest energy forms of the TAR-*tat*12 complex, as determined from AutoDock calculations. Tat12.10 (blue) and Tat12.12 (red) span both the major and minor grooves, near the bulge. Tat12.13 (green) is bound solely in the major groove.
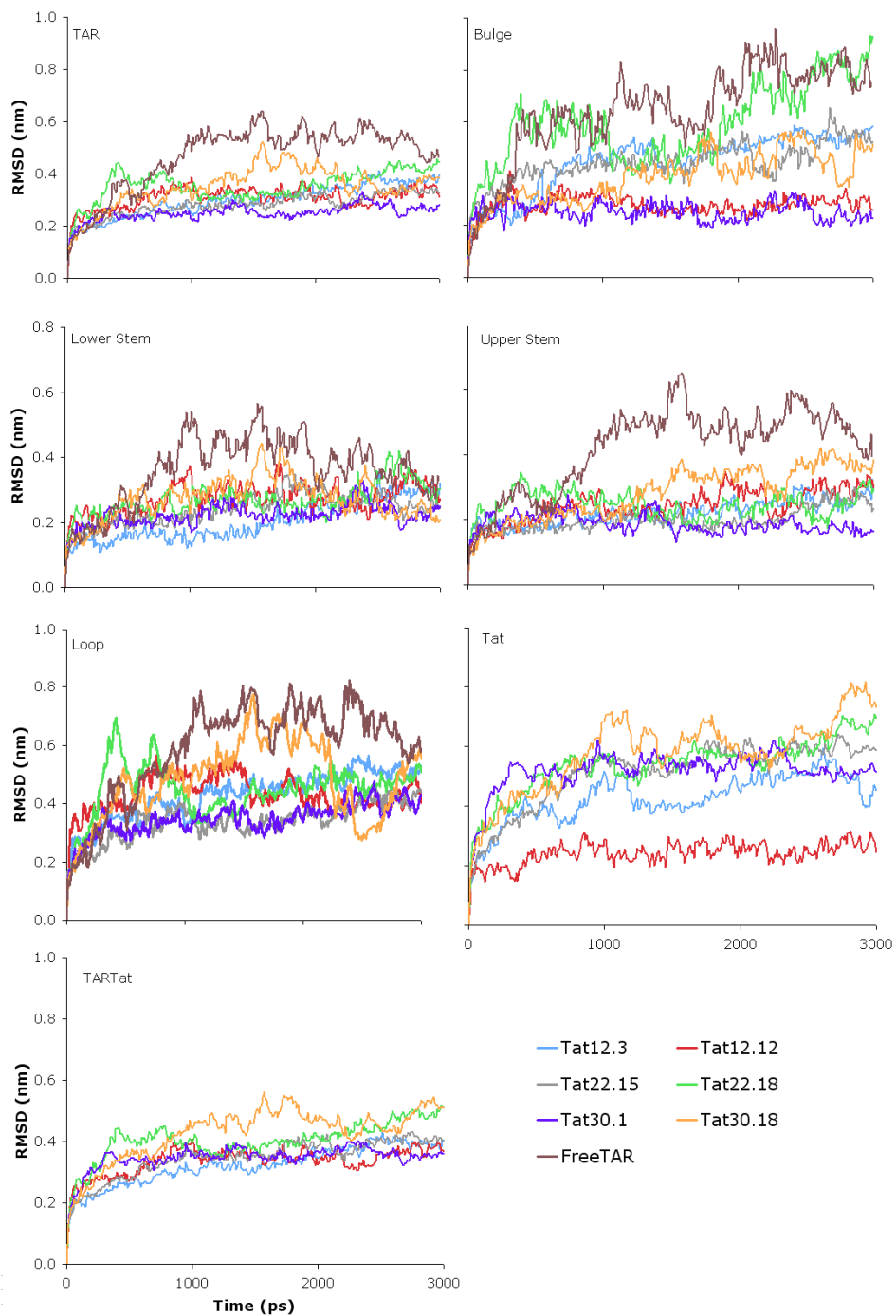
Fig. S.3 - Root mean square deviations of various elements of the TAR-*tat* system, with respect to the initial position, for the 3-ns simulations of Str1.
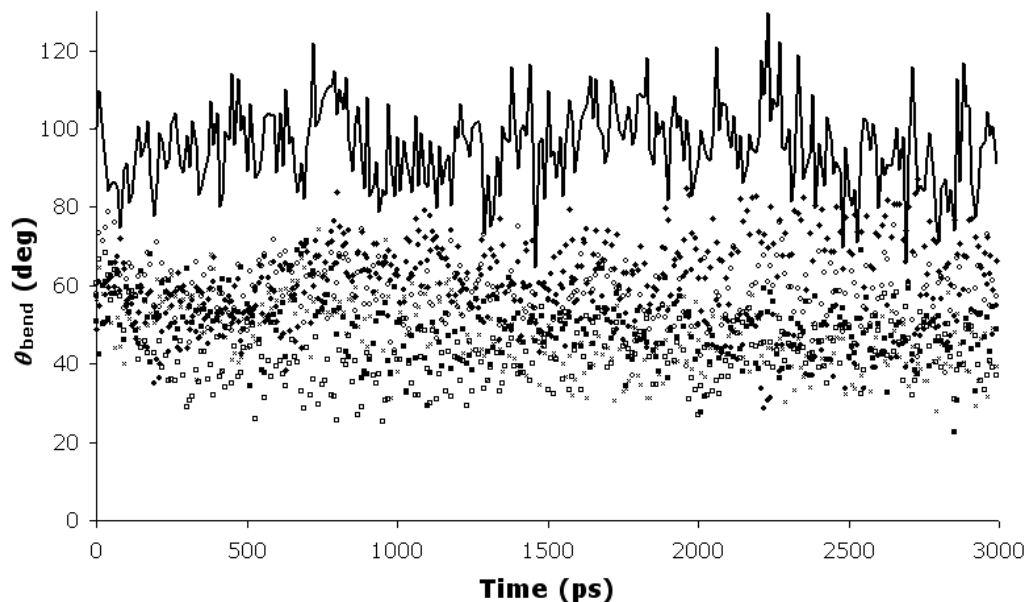
Fig. S.4 - Bend angle between the lower and upper stems for bound and unbound TAR. The solid line shows unbound apoTAR and the shapes represent the bound forms, as follows: Tat12.3 (♦), Tat12.12 (✕), Tat22.15 (●), Tat22.18 (○), Tat30.1 (□), Tat30.18 (■).
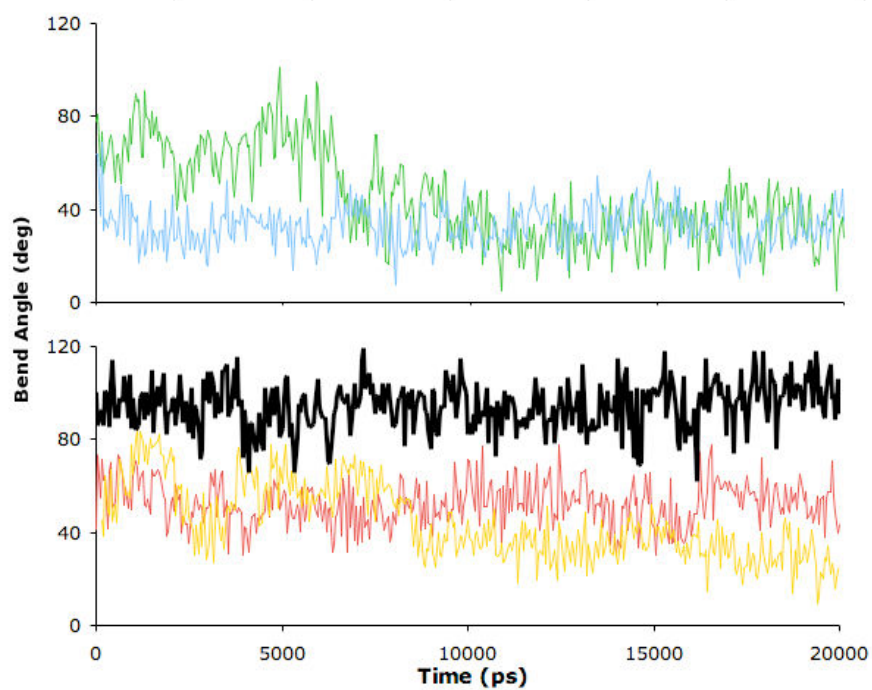
Fig. S.5 - Bend angle, in degrees, between the lower and upper stem of TAR RNA, over the entire simulation runs. Green is Tat12.10, blue is Tat12.13, red is Tat30.10, orange is Tat30.13, and black is unbound TAR.
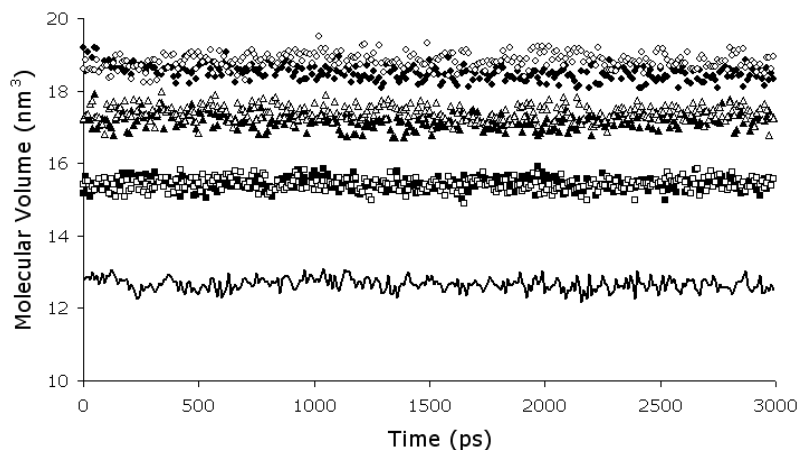
Fig. S.6 - Molecular volume as a function of simulation time for the different
TAR-*tat* and unbound TAR macromolecules. The solid line shows unbound
apoTAR and the shapes represent the bound forms, as follows: Tat12.3 (♦),
Tat12.12 (✗), Tat22.15 (●), Tat22.18 (○), Tat30.1 (□), Tat30.18 (■).
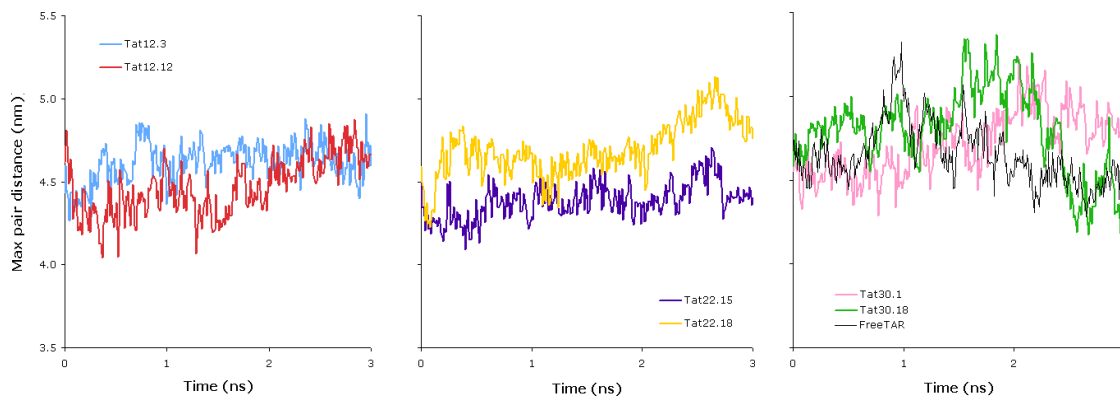
Fig. S.7 - Maximum atom-pair distances for the TAR RNA phosphorous atoms
over 3 ns simulations. The unbound TAR is shown in black in part c). The values
are recorded every 10 ps.

Fig. S.8 - Maximum atom-pair distances for TAR RNA over the 20-ns
simulations. The unbound TAR is shown in black in part b). The values are
extracted every 50 ps.

S5

III Tables

Table S.1 - Model estimates of viscoelasticity and interfacial slip for film relaxation time $\omega\tau = 0.3$ from Ref. 24. The units of μ_{NAv} are $g \cdot cm^{-1} \cdot s^{-2}$ and for s, $cm^2 \cdot s \cdot g^{-1}$. ([a]no solution found for $\omega\tau = 0.3$, so $\omega\tau = 0.22$ was used)

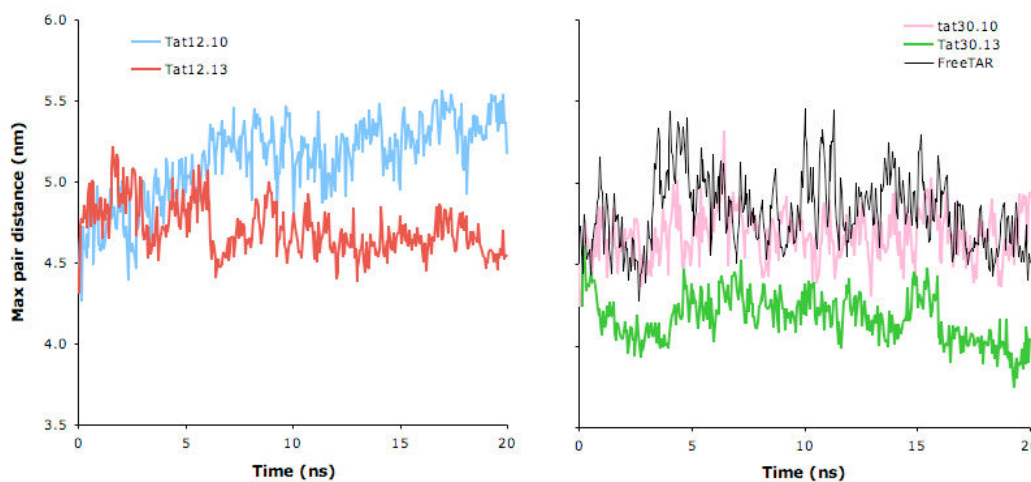|	Δf	ΔR	$\log(\eta_{NAv})$	$\log(\mu_{NAv})$	s_0 ($\times 10^{-5}$)
n1	-175	1.38	-1.90	6.36	6.96
n2	-170	0.99	-1.73	6.53	6.63
n6	-162	1.73	-2.04	6.23	6.25
n7	-214	1.82	-2.16[a]	6.26	9.10
n8	-188	0.78	-1.63[a]	5.27	9.65
n9	-182	1.77	-2.05	6.22	7.57
n10	-197	1.69	-2.13[a]	6.29	7.95
n11	-205	2.12	-2.25[a]	6.16	8.54
n12	-173	1.82	-2.06	6.21	7.02
n13	-178	1.67	-2.02	6.24	7.30
n14	-181	1.86	-2.07	6.19	7.57
n15	-164	1.54	-1.99	6.28	6.34
n16	-208	2.30	-2.14	6.14	8.96
n17	-189	1.61	-2.09[a]	6.31	7.83
n18	-157	1.48	-1.99	6.27	5.85
n19	-165	3.40	-2.38	5.89	7.06
n20	-179	1.15	-1.84	6.43	7.19
n21	-174	1.25	-1.87	6.40	6.94
n22	-170	2.46	-2.23	6.05	6.58
n23	-218	2.44	-2.18	6.10	9.66
n24	-178	0.79	-1.70[a]	5.19	9.33
n25	-197	2.60	-2.34[a]	6.07	8.18
n26	-176	1.47	-1.95	6.32	7.11
n27	-187	2.40	-2.20	6.07	7.65
		Mean	-2.0±0.2	6.1±0.3	8±1

Table S.2 – Average fitting of viscoelastic material parameters to experimental data for biotinylated TAR adsorption. The units of μ and η are $g \cdot cm^{-1} \cdot s^{-2}$ and $g \cdot cm^{-1} \cdot s^{-1}$, respectively. The last column shows the relaxation time, $\omega\tau = \omega\eta/\mu = G''/G'$.

Expt.	Δf (Hz)	ΔR (Ω)	$\log(\eta_{bTAR})$	$\log(\mu_{bTAR})$	$\omega\tau$
b1	-56.0	2.06	-2.38	5.86	0.32
b2	-54.1	1.81	-2.22	5.92	0.40
b6	-55.3	1.91	-2.40	5.81	0.34
b7	-35.4	0.46	-1.97	5.70	1.23
b8	-69.1	1.91	-2.01	5.81	0.84
b9	-63.9	2.39	-2.79	5.78	0.15
b10	-36.3	0.20	-1.90	5.69	1.48
b11	-42.0	0.78	-2.09	5.76	0.79
b12	-65.7	2.40	-2.87	5.79	0.12
b13	-64.1	2.41	-2.80	5.79	0.14
b14	-67.5	2.36	-3.00	5.78	0.09
b15	-56.6	1.94	-2.42	5.84	0.31
b16	-38.6	1.37	-2.19	5.69	0.75
b17	-70.2	2.20	-4.04	5.85	0.01
b18	-55.8	2.14	-2.46	5.80	0.30
b19	-62.8	2.12	-2.79	5.63	0.21
b20	-64.9	1.65	-2.64	5.96	0.14
b21	-62.6	1.97	-2.59	5.90	0.18
b22	-31.7	1.18	-2.21	5.61	0.85
b23	-43.2	1.25	-2.22	5.72	0.65
b24	-62.0	1.15	-1.91	5.59	1.75
b25	-36.2	0.99	-2.20	5.68	0.76
b26	-61.5	2.13	-2.59	5.85	0.20
b27	-26.5	1.47	-2.24	5.57	0.87
		Mean (SD)	-2.5 (0.5)	5.8 (0.1)	

Table S.3 – Changes in frequency and resistance for the adsorption of various length *tat* peptide to surface immobilised TAR RNA. The *Expt.* numbers are used for identification and the errors indicated in the averages are one standard deviation. *ta*8 and *ta*17 are not included, as the results for bTAR adsorption could not be modelled

tat length	*Expt.*	Δf (Hz)	ΔR (Ω)	Δf_{avg} (Hz)	ΔR_{avg} (Ω)
12	*ta*1	35.8	-3.9	32 ±5	-3.5 ±0.6
	*ta*2	28.4	-3.0		
20	*ta*6	34.6	-2.6	26 ±9	-2.7 ±0.9
	*ta*7	13.3	-1.8		
	*ta*9	33.4	-3.6		
	*ta*10	11.2	-1.4		
	*ta*11	23.1	-2.0		
	*ta*12	26.3	-3.0		
	*ta*13	25.5	-3.4		
	*ta*14	36.7	-3.8		
22	*ta*15	14.0	-2.3	15 ±2	-2.2 ±0.3
	*ta*16	17.6	-1.8		
	*ta*18	13.5	-2.5		
25	*ta*19	20.0	-2.2	18 ±4	-2.3 ±0.6
	*ta*20	21.9	-3.1		
	*ta*21	12.5	-2.2		
	*ta*22	18.6	-1.8		
27	*ta*23	5.4	-1.8	-0.2 ±8	-1.8 ±0.8
	*ta*24	0.0	-2.6		
	*ta*25	8.4	-1.4		
	*ta*26	-3.0	-2.5		
	*ta*27	-11.6	-0.7		
30	*ta*28	-24.9	-2.6	-21 ±6	-2.3 ±0.5
	*ta*29	-14.4	-1.8		
	*ta*30	-24.4	-2.6		

Table S.4 $-\alpha$ slip fitting results for the TAR-tat layer. Results are shown for inner slip and outer slip.

tat	Expt.	$|\alpha|_{outer}$	$\angle\alpha_{outer}$ (deg)	$|\alpha|_{inner}$	$\angle\alpha_{inner}$ (deg)
12	ta1	0.967	0.690	0.968	0.752
	ta2	0.974	0.503	0.975	0.548
20	ta6	0.972	0.512	0.972	0.570
	ta7	0.980	0.680	0.981	0.709
	ta8	0.977	0.439	0.977	0.475
	ta9	0.967	0.822	0.968	0.891
	ta10	0.983	0.579	0.984	0.600
	ta11	0.975	0.644	0.976	0.690
	ta12	0.972	0.803	0.973	0.860
	ta13	0.971	0.888	0.971	0.948
	ta14	0.965	0.852	0.965	0.926
22	ta15	0.980	0.763	0.980	0.798
	ta16	0.979	0.753	0.980	0.793
	ta17	0.970	0.673	0.971	0.727
	ta18	0.979	0.835	0.979	0.875
25	ta19	0.970	1.295	0.972	1.372
	ta20	0.974	0.739	0.975	0.780
	ta21	0.982	0.647	0.982	0.677
	ta22	0.976	0.889	0.978	0.936
27	ta23	0.981	1.053	0.982	1.082
	ta24	0.984	0.839	0.985	0.852
	ta25	0.980	0.871	0.981	0.906
	ta26	0.984	1.067	0.985	1.089
	ta27	0.991	1.118	0.992	1.121
30	ta28	0.994	1.052	0.995	1.040
	ta29	0.995	0.657	0.996	0.653
	ta30	0.995	1.026	0.995	1.014

Table S.5 – Updated fitting of viscoelastic material parameters to experimental data for biotinylated TAR adsorption, included TAR size computed from MD simulations. The units of μ and η are g·cm^{-1}·s^{-2} and g·cm^{-1}·s^{-1}, respectively. The last column shows the relaxation time, $\omega\tau = \omega\eta/\mu = G''/G'$.

Expt.	Δf (Hz)	ΔR (Ω)	$\log(\eta_{bTAR})$	$\log(\mu_{bTAR})$	$\omega\tau$
b1	-56.0	2.06	-2.08	5.78	0.75
b2	-54.1	1.81	-1.98	5.80	0.93
b6	-55.3	1.91	-2.13	5.75	0.73
b7	-35.4	0.46	-1.96	5.51	1.91
b8	-69.1	1.91	-1.95	5.63	1.43
b9	-63.9	2.39	-2.28	5.78	0.48
b10	-36.3	0.20	-1.92	5.47	2.31
b11	-42.0	0.78	-2.02	5.63	1.29
b12	-65.7	2.40	-2.29	5.79	0.46
b13	-64.1	2.41	-2.27	5.79	0.48
b14	-67.5	2.36	-2.32	5.80	0.42
b15	-56.6	1.94	-2.11	5.77	0.72
b16	-38.6	1.37	-2.10	5.59	1.16
b17	-70.2	2.20	-2.28	5.87	0.39
b18	-55.8	2.14	-2.16	5.76	0.68
b19	-62.8	2.12	-2.44	5.65	0.45
b20	-64.9	1.65	-2.04	5.90	0.64
b21	-62.6	1.97	-2.09	5.85	0.63
b22	-31.7	1.18	-2.14	5.53	1.22
b23	-43.2	1.25	-2.11	5.63	1.05
b24	-62.0	1.15	-1.95	5.38	2.61
b25	-36.2	0.99	-2.11	5.58	1.15
b26	-61.5	2.13	-2.15	5.82	0.60
b27	-26.5	1.47	-2.16	5.50	1.22
		Mean (*S.D.*)	-2.1 (0.1)	5.7 (0.1)	